Spectral and Structural Characterization of 5,6-Chrysenequinone Diimine Complexes of Rhodium(III): Evidence for a pH-Dependent Ligand Conformational Switch

Brian A. Jackson, Lawrence M. Henling, and Jacqueline K. Barton*

Division of Chemistry and Chemical Engineering, California Institute of Technology, Pasadena, California 91125

Received July 12, 1999

Rhodium(III) complexes containing 9,10-phenanthrenequinone diimine (phi) ligands have been broadly applied for the construction of DNA binding and recognition molecules, and more recently, derivatives containing the 5,6-chrysenequinone diimine (chrysi) ligand have been shown specifically to recognize base mismatches in DNA. Here the structural properties of $[Rh(bpy)_2(chrysi)]Cl_3$ and spectroscopic properties of derivatives are examined and compared to those of phi complexes of rhodium. Although similar in many respects, phi and chrysi complexes display distinctly different protonation behavior. The pK_a values of chrysi complexes are as much as 1 unit lower than analogous phi compounds, and visible spectra of the chrysi complexes differ markedly from the phi counterparts in acidic but not basic solution. This protonation behavior is traced to the presence of a steric clash between a proton on the aromatic ring of the chrysi ligand and the acidic immino proton of the metal complex. In avoidance of this steric clash, a significant disruption in the planarity of the chrysi ligand is evident crystallographically in the structure of $[Rh(bpy)_2(chrysi)]Cl_3 \cdot 3CH_3CN \cdot 2H_2O$ (triclinic crystal system, space group $P\bar{1}$ (No. 2), $Z = 2$, $a = 9.079(3)$ Å, $b = 10.970(3)$ Å, $c = 21.192(8)$ Å, $\alpha = 86.71(3)°$, $\beta = 89.21(3)°$, $\gamma = 78.58(3)°$, $V = 2065.4(12)$ Å^3). Phi complexes, lacking the additional aromatic ring, require no similar distortion from ligand planarity. NMR spectra support this pH-dependent structural distortion for the chrysi complex. Rhodium complexes of chrysenequinone diimine, therefore, not only represent new DNA binding molecules targeted to mismatches but also provide an illustration of a pH "gated" ligand conformational switch.

Introduction

Metallointercalators have been shown to be valuable probes of DNA structure and reactivity.[1] Our laboratory has focused on studies of rhodium(III) complexes containing the phenanthrenequinone diimine (phi) ligand in an effort to design complexes which bind to DNA with site-specificity.[2] These compounds bind to DNA by intercalation of the planar aromatic surface of the phi into the base stack; this interaction provides a high level of sequence neutral binding affinity for the nucleic acid. The intercalative binding mode in combination with the octahedral geometry and kinetic inertness of the Rh(III) center provides a stable and rigid framework on which to place chemical functionalities in defined positions in three-dimensional space. Thus, it has become possible to construct a family of DNA recognition molecules using the octahedral scaffolding of the metallointercalator.[1−6] Furthermore, these complexes have been demonstrated, upon photoactivation, to promote direct strand cleavage by hydrogen atom abstraction from a DNA sugar at their binding site.[7] Other metallointercalators have been found to be useful as luminescent probes of DNA,[8] but the combination of structural and photochemical properties has made phenanthrenequinone diimine complexes of rhodium(III) ideal for the design of novel DNA recognition agents.

In addition to complexes based on the phi ligand, we have recently become interested in the synthesis of rhodium complexes with other quinone diimine intercalating ligands (Figure 1).[9] Unlike the phi complexes, where the intercalating ligand provides sequence neutral binding to DNA for the delivery of other recognition elements, alternate quinone diimine ligands may make it possible to confer binding specificity as part of DNA intercalation. In particular, complexes containing the sterically bulky 5,6-chrysenequinone diimine ligand have been shown to confer binding specificity on destabilized regions of the DNA helix, particularly those surrounding DNA base mismatches.[10] These complexes are unique among small DNA-

* To whom correspondence should be addressed.

(1) Erkkila, K. E.; Odom, D. T.; Barton, J. K. *Chem. Rev.* **1999**, *99*, 2777. Lippard, S. J. *Acc. Chem. Res.* **1978**, *11*, 211. Chow, C. S.; Barton, J. K. *Methods Enzymol.* **1992**, *212*, 219. Armitage, B. *Chem. Rev.* **1998**, *98*, 1171.

(2) Johann, T. W.; Barton, J. K. *Philos. Trans. R. Soc. A* **1996**, *354*, 299−324.

(3) Terbrueggen, R. H.; Barton, J. K. *Biochemistry* **1996**, *34*, 8227−8234.

(4) Terbrueggen, R. H.; Johann, T. W.; Barton, J. K. *Inorg. Chem.* **1998**, *37*, 6874−6883.

(5) (a) Sitlani, A.; Barton, J. K. *Biochemistry* **1994**, *33*, 12100. (b) Sitlani, A.; Dupureur, C. M.; Barton, J. K. *J. Am. Chem. Soc.* **1993**, *115*, 12589−90.

(6) (a) Krotz, A. H.; Kuo, L. Y.; Shields, T. P.; Barton, J. K. *J. Am. Chem. Soc.* **1993**, *115*, 3877. (b) Shields, T. P.; Barton, J. K. *Biochemistry* **1995**, *34*, 15049−15056. (c) Krotz, A. H.; Hudson, B. P.; Barton, J. K. *J. Am. Chem. Soc.* **1993**, *115*, 12577.

(7) Sitlani, A.; Long, E. C.; Pyle, A. M.; Barton, J. K. *J. Am. Chem. Soc.* **1992**, *114*, 2303−2312.

(8) (a) Murphy, C. J.; Barton, J. K. *Methods Enzymol.* **1993**, *226*, 576. (b) Friedman, A. E.; Chambron, J.-C.; Sauvage, J.-P.; Turro, N. J.; Barton, J. K. *J. Am. Chem. Soc.* **1990**, *112*, 4960. (c) Moucheron, C.; Kirschdemesmaeker, A.; Kelly, J. M. *J. Photochem. Photobiol. B* **1997**, *40*, 91. (d) Moucheron, C.; Kirsch-De MesMaeker, A.; Choua, S. *Inorg. Chem.* **1997**, *36*, 584. (e) Jacquet, L.; Kirsch-De MesMaeker, A *J. Chem. Soc., Faraday Trans.* **1992**, *88*, 2471. Stoeffler, H. D.; Thornton, N. B.; Temkin, S. L.; Schanze, K. S. *J. Am. Chem. Soc.* **1995**, *117*, 7119. (f) Yam, V. W.-W.; Lo, K. K.-W.; Cheung, K.-K.; Kong, R. Y.-C. *J. Chem. Soc., Dalton Trans.* **1997**, *3*, 2067.

(9) Mürner, H.; Jackson, B. A.; Barton, J. K. *Inorg. Chem.* **1998**, *37*, 3007−3012.

10.1021/ic990824l CCC: $18.00
Published on Web 12/03/1999

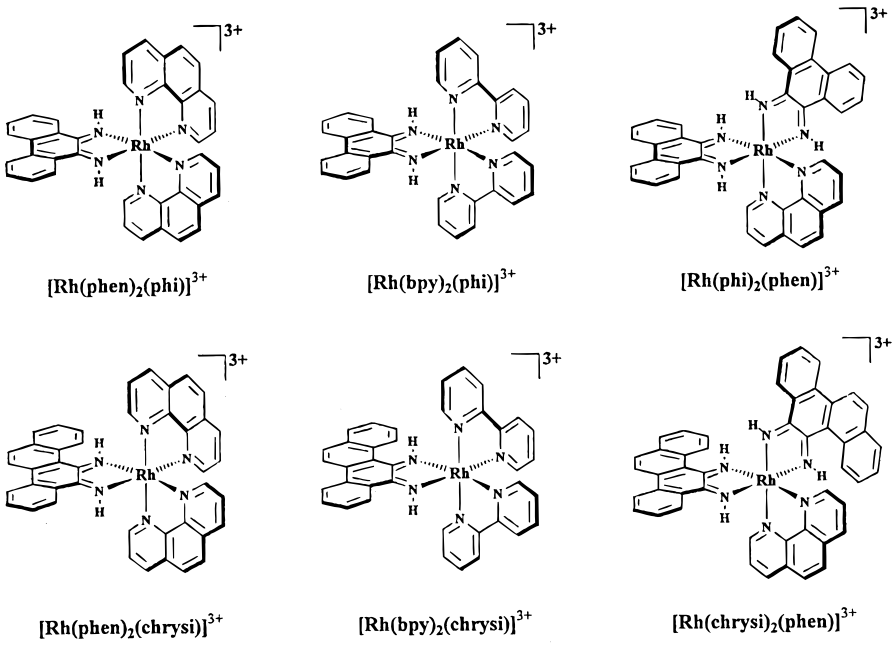

Figure 1. Structures of the complex ions: $[Rh(bpy)_2(chrysi)]^{3+}$; $[Rh(bpy)_2(phi)]^{3+}$; $[Rh(phen)_2(chrysi)]^{3+}$; $[Rh(phen)_2(phi)]^{3+}$; $[Rh(chrysi)_2(phen)]^{3+}$; $[Rh(phi)_2(phen)]^{3+}$.

binding molecules in that they not only recognize over 80% of the possible mismatch sites in DNA but also bind with high enough specificity to allow the discrimination of a single mismatch in multikilobase DNA fragments.[11] As part of the characterization of these compounds in their application as DNA cleavage reagents, significant differences became apparent in the protonation behavior of these complexes from their phenanthrenequinone diimine parent compounds. These differences, which are described in detail here, revealed that these complexes exhibit significant structural changes depending on the protonation state of the imino nitrogen on one side of the asymmetric quinone diimine ligand.

Experimental Section

Instrumentation and Materials. The complexes utilized in this study, bis(2,2′-bipyridyl)(5,6-chrysenequinone diimine)rhodium(III) trichloride ($[Rh(bpy)_2(chrysi)]Cl_3$), bis(2,2′-bipyridyl)(9,10-phenanthrenequinone diimine)rhodium(III) trichloride ($[Rh(bpy)_2(phi)]Cl_3$), bis(1,10-phenanthroline)(5,6-chrysenequinone diimine)rhodium(III) trichloride ($[Rh(phen)_2(chrysi)]Cl_3$), bis(1,10-phenanthroline)(9,10-phenanthrenequinone diimine)rhodium(III) trichloride ($[Rh(phen)_2(phi)]Cl_3$), bis(5,6-chrysenequinone diimine)(1,10-phenanthroline)rhodium(III) trichloride ($[Rh(chrysi)_2(phen)]Cl_3$), and bis(9,10-phenanthrenequinone diimine)-(1,10-phenanthroline)rhodium(III) trichloride ($[Rh(phi)_2(phen)]Cl_3$), were made and purified as previously described.[9] All other reagents were obtained from various commercial sources and used as received without further purification. The bipyridine-d_8 was generously provided by P. Belser and A. von Zelewsky. NMR spectra were recorded on a GE-300 MHz NMR or an AMX 500 MHz NMR. Absorption spectra were recorded on a Beckman DU 7400 spectrophotometer.

Measurement of pH-Dependent Optical Changes. A solution of one phi or chrysi complex (100−150 mL, 0.5−1.2 absorbance units at maximum) was prepared in a 250 mL beaker equipped with mechanical stirring. The solution was titrated with microliter aliquots of concentrated stocks of either sodium hydroxide or hydrochloric acid and the pH monitored by an internal electrode. The pH of the solution was adjusted from approximately 2.0 to 12.0; the titration was then reversed.

Table 1. Crystal Data and Structural Analysis Results for $[Rh(bpy)_2(chrysi)]Cl_3{\cdot}3CH_3CN{\cdot}2H_2O$

formula	$C_{44}H_{41}Cl_3N_9O_2Rh$
fw	937.13
cryst system	triclinic
space group	$P\bar{1}$(No. 2)
Z	2
cell params	
a (Å)	9.079(3)
b (Å)	10.970(3)
c (Å)	21.192(8)
α (deg)	86.71(3)
β (deg)	89.21(3)
γ (deg)	78.58(3)
V (Å^3)	2065.4(12)
cryst size (mm)	0.13 × 0.22 × 0.33
habit	block
ρ_{calc} (g cm^{-3})	1.507
μ (cm^{-1})	6.57
F_{000}	960
radiation (λ, Å)	Mo Kα (0.7107)
2θ range (deg)	3−50
temp (K)	85
no. of reflcns measd, indepdt reflcns	15 224, 7250
GOF_{merge}	0.98 for 7250 multiples
final $R(F_o)$ [6433 reflections with $F_o^2 > 3\sigma(F_o^2)$]	0.026
final $R(F_o)$ [7006 reflections with $F_o^2 > 0$]	0.063
final goodness of fit (728 params, 7250 reflcns)	1.81
$\Delta\rho_{max}$ (e Å^{-3}), $\Delta\rho_{min}$ (e Å^{-3})	0.75, −0.56

At multiple points during the titration, an aliquot of the solution was removed and its absorption spectrum measured. The aliquot was then returned to the titration reservoir and the experiment continued. An optical titration curve was constructed from the absorbance readings at a single wavelength for each complex and the pK_a of the compound determined from the inflection point of the curve.

Single-Crystal X-ray Diffraction Structural Characterization of $[Rh(bpy)_2(chrysi)]Cl_3{\cdot}3CH_3CN{\cdot}2H_2O$. A sample of cation-exchange-purified racemic metal complex crystallized from acetonitrile as dark brown triclinic blocks. A single crystal was mounted with Paratone-N on a CAD-4 diffractometer. The crystal and data collection details are summarized in Table 1. CRYM programs were used for data processing.[12] Reflections which did not agree well in a preliminary merging were recollected. No decay or absorption corrections were needed.

(10) Jackson, B. A.; Barton, J. K. *J. Am. Chem. Soc.* **1997**, *119*, 12986−12987.
(11) Jackson, B. A.; Alekseyev, V. Y.; Barton, J. K. *Biochemistry* **1999**, *38*, 4655−4662.

Individual backgrounds were replaced with a background function of 2θ derived from the backgrounds of reflections with $I < 3\sigma(I)$. Lorentz and polarization factors were applied, and the multiples were merged in point group $\bar{1}$; 13 outliers were deleted from the final dataset. Weights were calculated as $1/\sigma^2(F_o^2)$; variances ($\sigma^2(F_o^2)$) were derived from counting statistics plus an additional term, $(0.014I)^2$. Variances of the merged data were obtained by propagation of error plus an additional term $(0.014\langle I\rangle)^2$.

The structure was solved with direct methods in SHELXS-86.[13] One of the chloride ions occupies two sites, which are also partially occupied by a water molecule. One of the three acetonitrile molecules is disordered. On the basis of early refinement cycles, the populations of all these atoms were fixed at 0.5. The hydrogen atoms on one of the half-occupancy water molecules and one hydrogen atom on the disordered acetonitrile could not be reliably located and were not included in the model. All non-hydrogen atoms were refined anisotropically; all included hydrogen atoms were refined isotropically. Both atoms occupying the mixed Cl/O sites were refined independently. Refinement was by full-matrix least squares on F_o^2 using CRYM programs.[12]

pH Titration of [Rh(bpy-d_8)$_2$(chrysi)]Cl$_3$ by 1D-^{1}H NMR Spectroscopy. A pH titration was performed on [Rh(bpy-d_8)$_2$(chrysi)]Cl$_3$ using proton NMR. The complex with deuterated ancillary ligands was used so the multiple bipyridine proton signals would not obscure chrysi signals of interest. A sample of the complex in 90/10 H_2O/D_2O was studied using the WATERGATE gradient solvent suppression.[14] The pH of the solution was monitored with an external pH meter equipped with an appropriate probe. The pH was titrated from 1.5 to 9.6 with small aliquots of concentrated aqueous HCl and NaOH solutions between 1D spectra acquisition.

Results and Discussion

Spectroscopic Features of Phenanthrenequinone Diimine and Chrysenequinone Diimine Complexes. The electronic spectra of phenanthrenequinone diimine compounds of rhodium(III) have been extensively studied.[7,15,16] The absorbance characteristics of these compounds, containing features in both the ultraviolet and visible regions of the spectrum, have been broadly characterized as combinations of the spectra of the component ligands. Not unexpectedly, the electronic spectra of chrysi complexes of Rh(III) are analogous in structure to those of their parent phi compounds. As a result, the spectrum can be broadly characterized as consisting of contributions from the phen or bpy ancillary ligands in the ultraviolet region and visible transitions associated with the diimine intercalator. Although very similar in the region of the spectrum assigned to the ancillary ligands, significant differences between analogous phi and chrysi compounds are apparent in the visible transitions ascribed to their respective quinone diimine ligands. An example of these differences, for the $[Rh(bpy)_2(phi)]^{3+}/[Rh(bpy)_2(chrysi)]^{3+}$ pair, is shown as Figure 2. The spectral features in the visible region of the chrysi spectrum are broader and extend to longer wavelength than those in the corresponding phi complex. For comparison the spectrum of chrysenequinone shows an absorption maximum at 400 nm; the diimine ligands themselves are unstable in solution. The divergence in absorbance characteristics between the phi and chrysi complexes become even more dramatic at acidic pH. The spectral changes which occur for the bis(2,2′-bipyridyl) chrysi and phi compounds and of the 1,10-phenanthroline bis(chrysi) or bis(phi) compounds upon titration are shown as Figures 3 and 4, respectively.

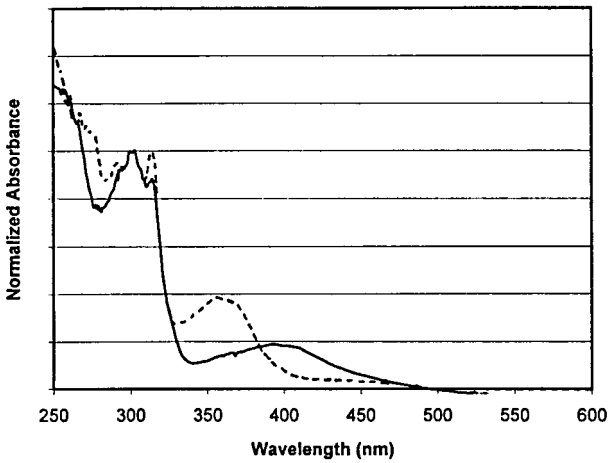

Figure 2. Comparison of the absorption spectra of $[Rh(bpy)_2(chrysi)]^{3+}$ and $[Rh(bpy)_2(phi)]^{3+}$ in 100 mM Tris at pH 8.0. Note the broader envelope of visible absorbance observed in the chrysi complex compared to the corresponding phi compound.

For complexes containing the phenanthrenequinone diimine ligands, the effect of pH differences on the absorption spectrum is relatively straightforward. In the bis(2,2′-bipyridyl) case, as solution pH is increased, hypochromicity is observed in the visible absorbance along with a shift to the blue; additional changes in intensity are observed in the ultraviolet transitions. In the bis(phi) complex, a similar blue shift and hypochromicity is observed in the visible absorbance in addition to the appearance of a broad absorbance "tail" extending into the red. In contrast, the changes which occur in the chrysi complexes are much more complex. In the case of $[Rh(bpy)_2(chrysi)]^{3+}$, at least two separate absorbance peaks are visible in acidic solution instead of the single feature observed for the corresponding phi compound. Like the phi complex, the absorbance does blue shift as the pH is increased; in this case, however, it does so with significant changes in profile. In addition to the change in the absorption maximum, the two (or more) separate features coalesce into a single peak centered in the 360−370 nm region. Similar changes are observed in the case of $[Rh(chrysi)_2(phen)]^{3+}$, where the broad absorbance envelope observed at acidic pH also forms a somewhat simpler peak structure which is shifted to higher energy.

Thus, for both chrysi complexes, their absorbance characteristics diverge markedly from their phi-containing counterparts only at acidic pH. Significantly, as the solution pH is increased, the spectra of the two compounds converge to very similar patterns.

pK_a Measurement by Spectroscopic Titration. The significant differences in the spectral behaviors observed for phi and chrysi complexes at different solution pH values led to further interest in the acid/base properties of these compounds. The pK_a values of the complexes were therefore determined from spectroscopic titrations analogous to those included in Figures 3 and 4. Plotting the change in absorbance observed at a single wavelength in these spectral titrations as a function of pH provides a facile method for construction of a titration curve for the imino protons on the phi or chrysi ligand.[15] In the case of phi complexes, quantitative potentiometric titrations had shown that, for $[Rh(phen)_2(phi)]^{3+}$, only the first imino proton dissociates in the pH range examined.

Analysis of titration data for both phi- and chrysi-containing complexes revealed that, in addition to the significant differences

(12) Duchamp, D. J. *Abstracts of Papers*, American Crystallographic Association Meeting, Bozeman, MT, 1964; Paper B14, pp 29−30.
(13) Sheldrick, G. M. *Acta Crystallogr.* **1990**, *A46*, 467−473.
(14) Piotto, M.; Saudek, V.; Skenar, V. *J. Biomol. NMR* **1992**, *2*, 661−665.
(15) Pyle, A. M.; Chiang, M. Y.; Barton, J. K. *Inorg. Chem.* **1990**, *29*, 4487−4495.
(16) Krotz, A. H.; Kuo, L. Y.; Barton, J. K. *Inorg. Chem.* **1993**, *32*, 5963−5974.

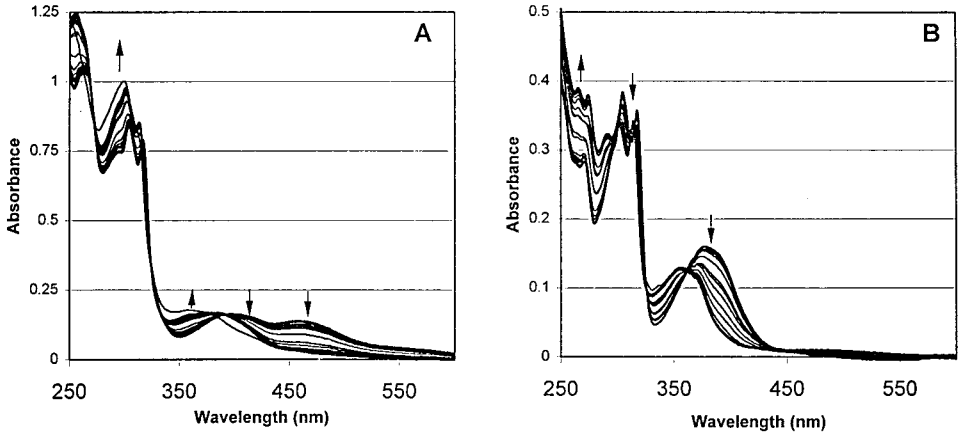

Figure 3. Spectral changes which occur upon titration of a solution of (A) $[Rh(bpy)_2(chrysi)]^{3+}$ and (B) $[Rh(bpy)_2(phi)]^{3+}$ between pH 2.5 and pH 10.5. For both molecules, the visible absorbance transition ascribed to the quinone diimine ligand shifts to the blue and loses intensity with increasing pH (see arrows). The spectral structure of the two compounds are quite different at low pH; as pH increases, however, the spectra of the two compounds converge to become much more similar.

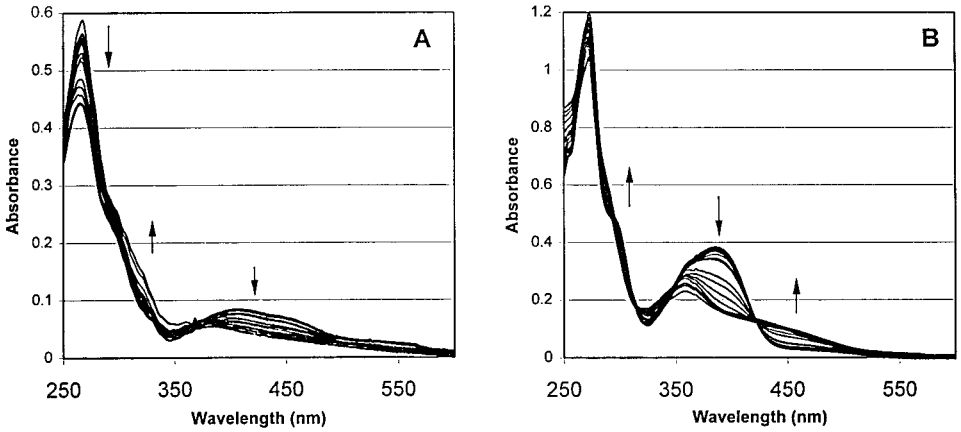

Figure 4. Spectral changes which occur upon titration of a solution of (A) $[Rh(chrysi)_2(phen)]^{3+}$ and (B) $[Rh(phi)_2(phen)]^{3+}$ between pH 2.5 and pH 10. For both molecules, the visible absorbance transition ascribed to the quinone diimine ligand shifts to the blue and loses intensity with increasing pH; appearance of a "tail" in the spectrum to the red is also observed (see arrows). As was observed in the previous figure, the spectral structures of the two compounds differ at low pH; as pH increases, however, the spectra of the two compounds converge to become much more similar.

Table 2. pK_a Values for phi and chrysi Complexes of Rh(III) Determined by Spectrophotometric Titration[a]

$[Rh(phen)_2(phi)]^{3+}$	6.0	$[Rh(bpy)_2(chrysi)]^{3+}$	5.2
$[Rh(phen)_2(chrysi)]^{3+}$	4.9	$[Rh(phi)_2(phen)]^{3+}$	6.7
$[Rh(bpy)_2(phi)]^{3+}$	5.8	$[Rh(chrysi)_2(phen)]^{3+}$	5.5

[a] Titrations performed at ambient temperature (~25 °C) in deionized water. Error in the reported values is estimated at +/−0.2 by comparison of repeated trials.

in spectral characteristics observed at acidic pH (Figures 3 and 4), the pK_a values measured for chrysi-containing complexes (Table 2) were systematically lower than their phi counterparts. In all cases, the pK_a value measured for the chrysi containing complexes is between 0.6 and 1.2 units below that of the corresponding phi complex. We expect that the stoichiometry of proton loss matches that for the phi complexes. The imino pK_a values for both the phi and chrysi complexes are understandable in comparison to those of other Ru and Rh diimine complexes containing bpy as ancillary ligands; for example for $[Ru(bpy)_2(bibenzimidazole)]^{2+}$, the p$K_a$ for the first imino proton is 6.5.[17] This depression in pK_a of the chrysi compounds, compared to their phi counterparts, when combined with the variance in pH dependence of the spectral structures themselves, suggested that significantly different environments must exist for the protons associated with the imino nitrogens in chrysi complexes. Molecular modeling studies suggested that this difference in acid−base behavior could be traced directly to the presence of the additional aromatic ring in the chrysene ligand through steric rather than electronic interaction. This hypothesis was confirmed crystallographically.

Crystallographic Characterization of $[Rh(bpy)_2(chrysi)]Cl_3$. Although crystal structures have previously been determined of phi complexes of rhodium-[16,18] and ruthenium-containing phi ligands,[15] the novelty of the chrysenequinone diimine ligand made the molecular structure of a representative complex containing chrysi of considerable interest. An ORTEP drawing of the structure of the complex ion $[Rh(bpy)_2(chrysi)]^{3+}$ is included (Figure 5).[19]

The structure of the chrysi complex is perhaps best compared to that of $[Ru(bpy)_2(phi)](BF_4)_3$;[15] crystal structures of phi complexes of Rh(III) have also been determined but with saturated amine ligands in the ancillary sites.[16,18,20] Compared

(17) (a) Hage, R.; Dijkhuis, H. J.; Haasnoot, J. G.; Prins, R.; Reedijk, J.; Buchanan, B. E.; Vos, J. G. *Inorg. Chem.* **1988**, *27*, 2185. (b) Haga, M.; Ano, T.; Ishizaki, T.; Kano, K.; Nozaki, K.; Ohno, T. *J. Chem. Soc., Dalton* Trans. **1994**, 263. (c) Furuhashi, A.; Endo, K.; Takagi, S.; Yoshino, Y. *Bull. Chem. Soc. Jpn.* **1991**, *64*, 298.
(18) Schaefer, W. P.; Krotz, A. H.; Kuo, L. Y.; Shields, T. P.; Barton, J. K. *Acta Crystallogr.* **1992**, *C48*, 2071−2073.
(19) Johnson, C. K. *ORTEPII*; Report ORNL-5138; Oak Ridge National Laboratory: Oak Ridge, TN, 1976.
(20) Krotz, A. H.; Barton, J. K. *Inorg. Chem.* **1994**, *33*, 1940−1947.

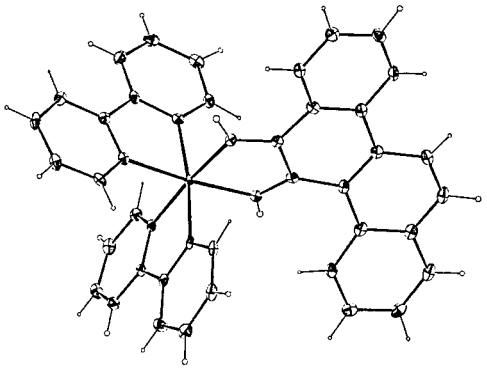

Figure 5. ORTEP plot of the complex ion $[Rh(bpy)_2(chrysi)]^{3+}$ from the X-ray structure of $[Rh(bpy)_2(chrysi)]Cl_3 \cdot CH_3CN \cdot 2H_2O$.[18]

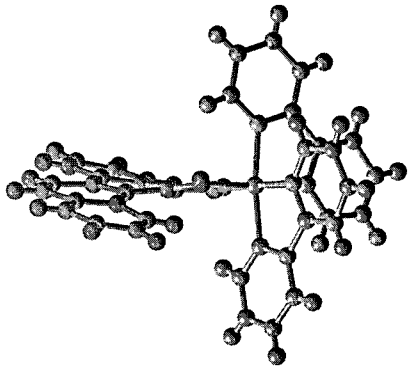

Figure 6. Side view of the crystal structure of the complex ion $[Rh(bpy)_2(chrysi)]^{3+}$. Note the severe distortion of the planarity of the chrysi ligand.

to the structure of $[Ru(bpy)_2(phi)](BF_4)_3$,[15] the bipyridyl ligands in the $[Rh(bpy)_2(chrysi)]^{3+}$ complex ion are essentially unchanged. As in the Ru(phi) complex, the general structure is a distorted octahedron with the N−Rh−N angles for ancillary ligand coordination (bipyridine N−Rh−bipyridine N) varying from 79.9(1) to 94.9(1)° and averaging 87.3°. Angles involving the chrysi nitrogens and bipyridine nitrogens are somewhat wider varying from 87.7(1) to 97.9(1)° and averaging 94.4°. The angle between the chrysi nitrogens themselves is the smallest N−Rh−N angle in the structure at 78.0(1)°. In addition, examination of the bond lengths in the structure shows that the Rh−(chrysi-N) bonds adopt a much shorter length (2.005(2) and 2.006(2) Å) than the Rh−(bpy-N) bonds (2.030(2)−2.039(2) Å). These trends in bond distances match those observed in the structures of Ru(phi) complexes, although their absolute values differ. In the structure of the ruthenium complex, although the Ru−(phi-N) bond lengths were almost identical to the observed Rh−(chrysi-N) distances (averaging 2.006(4) Å), the Ru−(bpy-N) distances were much longer (averaging 2.064(4) Å).[18]

With examination of the structure of the complex more closely, however, significant differences between the Ru(phi) compound and the Rh(chrysi) complex emerge which are directly relevant to the differences in acidity properties observed between phi and chrysi complexes. Unlike the Ru(phi) complex, which displays an essentially planar structure of the phi ligand, the chrysi intercalating ligand is severely distorted from planarity. Phi complexes of Rh(III) have also consistently shown full planarity in the phi ligand.[16,18,20] This distortion in the chrysi ligand is clearly observed in the view included as Figure 6.

We ascribe this distortion from planarity to a steric clash between the acidic proton on the imino nitrogen and the aromatic

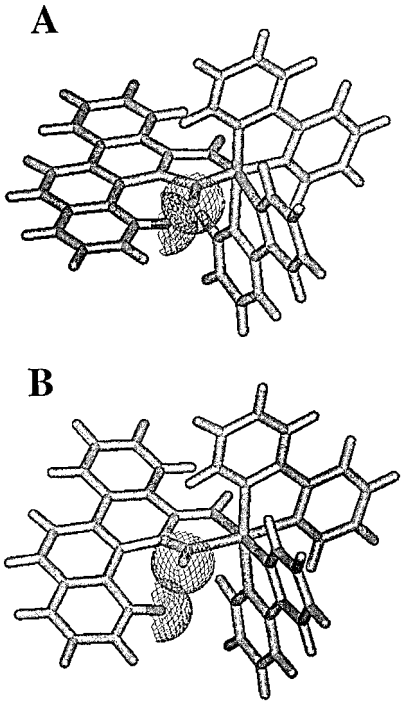

Figure 7. Comparison of a molecular model (A) of $[Rh(bpy)_2(chrysi)]^{3+}$ whose chrysenequinone diimine ligand has been forced into planarity with the crystal structure (B) of the same molecule. The van der Waals surfaces of the protons of interest are indicated with wire-frame mesh. In the model derived from crystal data, bond distances have been corrected to 1.08 and 1.00 Å for the C−H and N−H bonds, respectively, to compensate for the artificially short distances obtained crystallographically due to concentration of electron density away from the hydrogen atoms. Note that extensive overlap between the aromatic proton and the imino proton on the chrysi ligand occurs when the ligand is constrained in a planar geometry; this clash is greatly reduced by the deformation of the ligand.

proton which is directed back toward the rhodium center on the chrysene ring. In fact, the crystallographic data allowed the determination of hydrogen atom positions, which supports the need for such a distortion. The steric interaction between the two hydrogen atoms is graphically illustrated in Figure 7 which includes both a molecular model (panel A), where the chrysi ligand has been forced into planarity, and a view of the crystal structure (panel B) in its distorted state. It is clear that, to force the aromatic rings into planarity, significant overlap is required between the two atoms; the distortion observed in the crystal structure relieves this clash. In all the structures which have been previously determined of phi-containing compounds, where no aromatic hydrogens are positioned directly back toward the metal center and such a steric clash is not possible, no distortion of the quinone diimine ligand is observed.[15,16,18,20]

Beyond the characteristics of the complex itself, the crystal structure of $[Rh(bpy)_2(chrysi)]Cl_3 \cdot 3CH_3CN \cdot 2H_2O$ is also noteworthy for the extensive hydrogen-bonding network that exists within the crystal lattice. The three chloride ions and three acetonitrile and two water molecules form two hydrogen-bonding "strings" which traverse the unit cell (Supporting Information). The more defined bonding string is made up of a metal complex imino proton hydrogen bonded to a chloride ion which is bound to an ordered water which in turn is bound to the next chloride which bonds to the imino of the next complex. A second network of hydrogen bonds goes along the edges of the unit cell made up of the remaining chloride ion, the remaining water molecule, and the acetonitrile molecules. In addition to the hydrogen-bonding contacts which occur in the

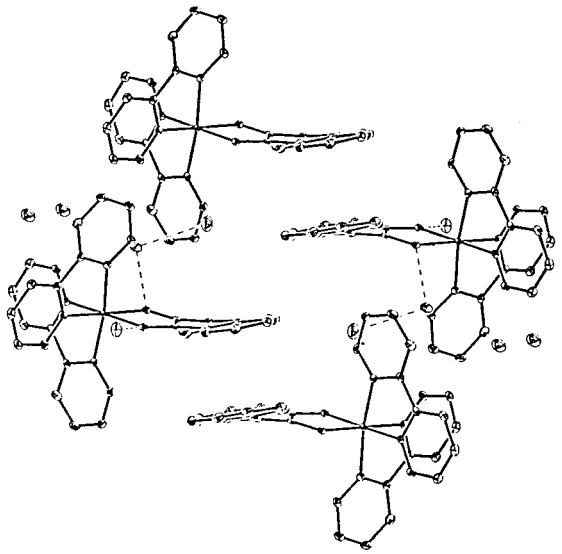

Figure 8. Side view of four molecules from the crystal structure of $[Rh(bpy)_2(chrysi)]Cl_3$. Note the positioning of the chrysi intercalating ligands above one another to participate in aromatic−aromatic stacking interactions.

crystal, there are also significant aromatic−aromatic stacking interactions stabilizing the structure despite the distortion in the chrysi ligand. These stacking contacts occur between the sides of the chrysi ligand not subject to the distortion and twisting (Figure 8). This partial overlap of the diimine intercalating ligands is similar to that observed in crystal structures of phi complexes.

pH Titration of $[Rh(bpy\text{-}d_8)_2(chrysi)]Cl_3$ by 1D-^{1}H NMR Spectroscopy. Examination of $[Rh(bpy)_2(chrysi)]^{3+}$ by proton NMR further supports this model of the conformational shift imposed on the chrysi ligand that is associated with deprotonation. The results of a pH titration performed on $[Rh(bpy\text{-}d_8)_2(chrysi)]Cl_3$ in 90/10 H_2O/D_2O are included as Figure 9. At low pH (bottom of Figure 9), distinct resonances can be discerned for each of the 10 aromatic protons on the chrysi intercalator. In contrast, under basic conditions (top of Figure 9), the resonances are far less dispersed and some are coincident with one another implying that, in this state, the protons are in more similar environments. This change is consistent with the proposed flattening of the twisted ligand shown in Figure 6.

The chemical shifts of protons in both the acidified and basic NMR samples also support this view of the compound's pH-dependent deformation. In the acidified spectrum, a set of three doublets are 0.5−1.0 ppm upfield from the remainder of the resonances. This positioning is consistent with these protons being torqued out of plane and, as a result, subject to less of the aromatic ring currents of the chrysene ring system. The rapid exchange broadening of these peaks (in addition to the other doublet labeled "A" in Figure 9) as the pH is increased is also consistent with their being near the acidic site on the metal complex and therefore more subject to the protonation/deprotonation equilibrium as the solution approaches the pK_a of the compound. Because of the multiplicity of the peaks (all doublets), these four protons are likely at positions 1, 4, 9, and 10 in Figure 9 (inset); although it is more difficult to determine candidate peaks for protons 2 and 3, they may be the large singlet at approximately 8.25 ppm which also shifts dramatically as the pH approaches the pK_a (5.2) of the complex. The single resonance which is observed shifted far downfield ("B" in Figure 9) is also consistent with this model. In the deprotonated, planar chrysi ligand, one proton will be very close to the deprotonated

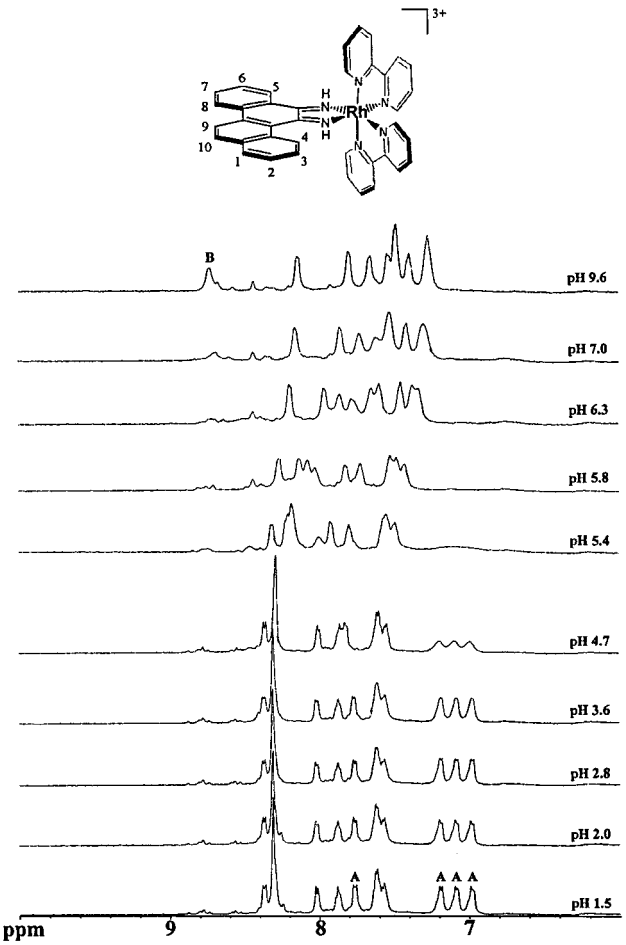

Figure 9. Results of a 1-D 500 MHz ^{1}H NMR pH titration of $[Rh(bpy\text{-}d_8)_2(chrysi)]Cl_3$ in 90/10 H_2O/D_2O using WATERGATE gradient solvent suppression. Note that the four doublets labeled "A" in the pH 1.5 (protonated) spectrum are shifted upfield from all resonances in the pH 9.6 (deprotonated) spectrum. In addition, these peaks, particularly the three near 7 ppm, are the most rapidly exchange broadened upon increasing the pH of the solution. Note also the single peak labeled "B" in the pH 9.6 spectrum. This peak, shifted far downfield from all the remaining peaks, is consistent with the placement of the proton at position 4 proximal to the imino anion of the deprotonated complex. Inset: Labeled $[Rh(bpy)_2(chrysi)]^{3+}$ for interpretation of NMR titration results.

imino anion. The presence of a single proton in this environment also supports the flattening of the chrysene ring with deprotonation.

Implications for DNA Binding. Since intercalative binding to DNA by metallointercalators requires the insertion of a *planar* aromatic ligand into the DNA base stack, it is possible that the geometric deformation of the chrysi ligand described here might be sufficient to prevent intercalation. The pK_a values for phi complexes of rhodium(III) have been observed to increase by between 0.5 and 1.3 units upon binding to DNA.[21] Given the low pK_a values observed for chrysi complexes in this study, it is unclear whether the complex would be protonated or deprotonated under the neutral to basic conditions customarily used for studies of nucleic acids. Certainly the protonation state of the metal complex is a consideration for studies performed under lower pH conditions. In fact, the selectivity of the chrysi complex for binding to mismatched DNA sites may be a result not only of the general expanse of chrysi complexes

(21) Turro, C.; Hall, D. B.; Chen, W.; Zuilhof, H.; Barton, J. K.; Turro, N. J. *J. Phys. Chem.* **1998**, *102*, 5708−5715.

compared to phi complexes but also of the ability of the distorted complex to bind only within a mismatched rather than matched and stacked site.

Conclusions

The results presented here provide a substantive picture of $[Rh(bpy)_2(chrysi)]^{3+}$, a novel complex based on a new quinone diimine ligand. The deformations observed in the crystal structure of the proton associated form of the complex not only serve as a structural explanation for the depressed pK_a values observed in all the compounds containing the chrysi ligand but also rationalize the differences between the absorbance characteristics of chrsyi complexes and their analogous phi compounds. Since at basic pH both ligands are planar and deprotonated, the spectral differences are minimal (Figures 2−4). At acidic pH, however, where the chrysi ligand is twisted out of plane, a splitting of the spectral transitions into multiple bands of significantly different maxima is observed. In the phi case, where no such structural changes are associated with protonation state, the spectrum retains its same overall structure and shifts much less dramatically in response to the change in pH. Complexes of chrysenequinone diimine are therefore not only of interest because of their potential as new DNA binding molecules targeted to mismatches but also as an example of molecules which contain a pH "gated" ligand conformational switch.

Acknowledgment. We gratefully acknowledge the financial support of the National Institutes of Health (Grant GM33309). B.A.J. acknowledges the NSF and the Parsons Foundation for predoctoral fellowships.

Supporting Information Available: Tables of the final atomic coordinates and displacement parameters, complete distances and angles, and hydrogen bonding details and figures showing additional views of aromatic stacking and hydrogen bonding in the crystal structure. This material is available free of charge via the Internet at http://pubs.acs.org.

IC990824L